Influence of the Post-Perovskite Transition on Thermal and Thermo-Chemical Mantle Convection

Paul J. Tackley

Institut für Geophysik, Department Erdwissenschaften, ETH Zürich, Switzerland

Takashi Nakagawa

Department of Earth and Planetary Sciences, Kyushu University, Fukuoka, Japan

John W. Hernlund[1]

Institut de Physique du Globe de Paris, France

Several studies have focused on the post-perovskite (PPV) transition's possible dynamical effect, as well as the complex seismological structures that may arise through the interplay of variations in temperature, composition and the PPV phase transition. Here these issues are explored using numerical models of thermal and thermo-chemical convection in various geometries including a three-dimensional spherical shell. A zero-, single- or double- crossing of the PPV phase boundary is observed depending on the temperatures of the CMB and deep mantle; this evolves with time as the core and mantle cool. The PPV transition has a minor effect on the dynamics and mantle temperature, mildly destabilizing the lower boundary layer and slightly increasing mantle temperature, depending on its depth relative to the thermal boundary layer. If piles of dense subducted MORB accumulate above the CMB then there is an anticorrelation between regions with a thick PPV layer and hot dense piles, but with a composition-dependent PPV transition this can change. Lateral variations in the occurrence of PPV are likely the dominant contributor to long-wavelength lateral shear-wave velocity heterogeneity in the deepest mantle, depending on some uncertain scaling parameters. The different contributions to seismic heterogeneity have different spectral slopes: temperature is "red", composition is "white" and PPV is intermediate. Theoretical considerations suggest that when compositional effects on the stability of PPV are taken into account, a large potential variety of complex behavior could occur, generating structures such as discontinuities, gaps or holes, and multiple (i.e., >2) crossings.

[1]Now at Department of Earth and Ocean Sciences, University of British Columbia, Vancouver, Canada.

Post-Perovskite: The Last Mantle Phase Transition
Geophysical Monograph Series 174

10.1029/174GM16

1. INTRODUCTION

As discussed extensively in this volume, mineral physics and ab initio calculations have shown that perovskite undergoes a phase change to post-perovskite (PPV) at pressure-temperature conditions near the top of the D" layer, 200-300 km above the core-mantle boundary (CMB) [*Hirose, et al.*, 2006; *Murakami, et al.*, 2004; *Oganov and Ono*, 2004; *Ono, et al.*, 2005; *Tsuchiya, et al.*, 2004a]. The density change of this phase transition is small, i.e., 1-2%, but the Clapeyron slope is relatively large, e.g., 3-13 MPa/K, so it might be expected that the phase transition could have significant effects on the lower thermal boundary layer of Earth's mantle. In addition to possible dynamical effects, it is important to understand the interaction between the phase transition and thermo-chemical structures in the CMB region because of the potentially complex seismological signatures that could be generated as well as understanding the expected distribution of PPV in the lowermost mantle.

Seismological observations of the CMB region indicate a great degree of heterogeneity and complexity (e.g., [*Lay and Garnero*, 2004]), for which several origins have been proposed, including compositional, thermal, melting- (e.g., [*Lay, et al.*, 2004]), and most recently, PPV related. Regarding compositional variations, a compositional change has often been invoked to explain the seismic "Lay" discontinuity observed at the top of D" in many areas [*Lay and Helmberger*, 1983], but the PPV transition is now the preferred explanation of this (even before PPV was discovered, it was argued that a strongly exothermic phase transition deflected upward by low temperatures fits the observations better than a chemical boundary, in which the boundary is deflected downward in regions of low temperature [*Sidorin, et al.*, 1999]). Nevertheless there are compelling reasons to believe that significant compositional variations exist, and play an important role in the deep mantle. Several global tomographic studies (e.g., [*Deschamps, et al.*, 2007; *Ishii and Tromp*, 1999; *Masters, et al.*, 2000; *Trampert, et al.*, 2004]) have argued that compositional variations are necessary to explain large-scale, high amplitude structures in the deep mantle, possibly consistent with numerical models of thermo-chemical mantle convection in which 'piles' of dense material form underneath large-scale upwellings [*McNamara and Zhong*, 2005; *Nakagawa and Tackley*, 2004c; *Tackley*, 1998; *Tackley*, 2002]. Seismological studies of local regions of the deep mantle indicate the need for vertical, sharp-sided structures, which have been argued to be compositional in origin [*Ni, et al.*, 2002; *Wen*, 2001; *Wen*, 2002], although phase changes and/or abrupt variations in elastic anisotropy can also induce strong lateral gradients in seismic velocity. Independently of seismic observations, geochemical observations indicate substantial chemical heterogeneity in the mantle, and compositionally-stratified slabs are continuously subducted and may well reach the CMB region where the different components could then undergo macro-segregation (e.g., [*Christensen and Hofmann*, 1994; *Olson and Kincaid*, 1991]).

The most likely explanation of deep mantle structure thus involves both compositional variations and the exothermic PPV phase change. The PPV phase change is affected by temperature and probably compositional variations. Due to its strongly positive Clapeyron slope combined with the large temperature gradients that are expected in the thermal boundary layer above the CMB, it has been proposed that perovskite is the stable phase at the CMB, resulting in a second ("double") crossing of the phase change, this time from PPV to perovskite, several tens of km above the CMB, and that such a feature has been found in the Cocos and Eurasia regions by comparing real data with synthetic seismograms generated for such a "double-crossing" scenario [*Hernlund, et al.*, 2005; *Thomas, et al.*, 2004a; *Thomas, et al.*, 2004b]. Recent seismological results support the presence of a PPV lens beneath the Cocos region [*van der Hilst, et al.*, 2007] and the mid-Pacific [*Lay, et al.*, 2006], though the latter study indicates the need for an important composition-dependence of the phase change depth (pressure) in order to explain the presence of PPV in both seismically fast and slow regions, consistent with some mineral physics studies [*Mao, et al.*, 2004; *Ono, et al.*, 2005; *Stackhouse, et al.*, 2006].

A number of numerical modeling studies have focused on the effect of the PPV transition on dynamics of thermal or thermo-chemical convection, and the structures that are generated by the interaction of PPV with temperature and sometimes compositional variations. In this paper we review these studies, focusing particularly on those by ourselves, and also present some new modeling results in spherical geometry. Finally, we offer a synthesis of possible thermo-chemical-PPV structures that might be observed in the CMB region, some of which are visible in presented models, others of which require more complex modeling to constrain.

2. MODEL

The modeling results illustrated in this paper, which are a mixture of previously-published results and new results, are all obtained with the numerical code STAG3D (e.g., [*Tackley*, 1993, 1996; *Tackley and Xie*, 2003]). This models thermal or thermo-chemical convection under the usual infinite Prandtl number approximation, and the compressible anelastic or Boussinesq approximation. The modeled geometry is either 2D cylindrical, 3D Cartesian, axisymmetric spherical, or 3D spherical-shell. 3D Cartesian was the original geometry of the code [*Tackley*, 1993]. In the cylindrical cases, the radii of the CMB and surface boundaries are rescaled such that surface area ratios match those in spherical geometry

[*van Keken*, 2001]. The option of treating a full 3D spherical-shell was recently added to the code using the "yin-yang" spherical grid [*Kageyama and Sato*, 2004], which combines two (longitude, latitude) patches, each spanning 270° in longitude by ±45° in latitude, to make a complete spherical shell.

The physical properties density, thermal expansivity, and thermal diffusivity are assumed to be dependent on depth, as given in [*Tackley and Xie*, 2003]. A summary of the values at the surface and CMB are given in Table 1. Viscosity is generally temperature- and depth-dependent, and can also be dependent on yield stress, and is specified later for each set of results presented. As the material properties of perovskite and post-perovskite (i.e., elasticity and thermodynamical properties) are similar [*Tsuchiya, et al.*, 2005; *Tsuchiya, et al.*, 2004b], it does not appear necessary to include a viscosity jump at this phase transition, although this could easily be incorporated in future if thought necessary. Some notable recent studies have included the temperature-dependence of thermal conductivity in addition to the pressure-dependence included here, including [*Matyska and Yuen*, 2005] who also included the post-perovskite phase change. Here, in order to not introduce too many complexities at once, we focus on the combined effect of compositional variations and the post-perovskite phase transition and leave temperature-dependent thermal conductivity to future studies.

Where stated, phase changes are incorporated at 400 km (+2.5 MPa/K) and 660 km (-2.5 MPa/K) in addition to the deep mantle PPV phase change. The version of the model used here is presented in great detail including all relevant equations in [*Xie and Tackley*, 2004a; 2004b]. An important change arises because of the large PPV Clapeyron slope and the possibility of crossing the PPV phase boundary twice or not at all [*Hernlund, et al.*, 2005], which makes it important to use a phase change treatment that allows these possibilities and correctly includes phase change deflection, rather than one in which the phase change is assumed to occur at a fixed depth. For this, a phase function approach is used,, based on that in [*Christensen and Yuen*, 1985]:

$$\Gamma_{ppv}(T,d) = 0.5 + 0.5\tanh\left(\frac{d - d_{ppv} - \gamma_{ppv}(T - T_{ppv})}{w}\right) \quad (1)$$

where Γ_{ppv} is the phase function for post-perovskite, which varies from 0 for perovskite to 1 for post-perovskite, T and d are temperature and depth, respectively, ($T_{\rm ppv}$, $d_{\rm ppv}$) is a point on the phase boundary, $\gamma_{\rm ppv}$ is the Clapeyron slope and w is the width of the phase transition, which for numerical reasons must be taken to be wider than realistic. Results presented later compare this treatment to the fixed-depth approximation used in preliminary results [*Nakagawa and Tackley*, 2004a]. The energy equation is identical to that given in previous studies (e.g., equation (3) of [*Xie and Tackley*, 2004a; 2004b]) but it is instructive to reproduce it here because the latent heat term is affected by the post-perovskite transition:

$$\bar{\rho}\bar{c}_p\left[\frac{\partial T}{\partial t} + \mathbf{u}\cdot\nabla T\right] = -Di_s\bar{\alpha}\bar{\rho}Tu_r + \nabla\cdot(\bar{k}\nabla T) + \bar{\rho}R_h + \frac{Di_s}{Ra}\tau_{ij}u_{i,j} + \bar{c}_p\frac{Di_sT}{\bar{\rho}}\sum_{i=1}^{nphase}P_i\frac{d\Gamma_i}{dz}u_r \quad (2)$$

where the barred quantities $\bar{\rho}, \bar{c}_p\bar{\alpha}, \text{and } \bar{k}$ are radius-dependent reference state properties density, heat capacity, thermal expansivity and thermal conductivity respectively, the calculation of which is defined in equations (11) to (14) of [*Tackley*, 1998]. Di_s is the surface dissipation number, *Ra* is the Rayleigh number defined using reference (generally surface) parameters, **u** is velocity, R_h is internal heating rate and τ_{ij} is the stress tensor. In the last (latent heat) term, P_i is the conventional phase buoyancy parameter for the i^{th} phase change and Γ_i is the phase function for the i^{th} phase change. Γ for the post-perovskite transition is given above and its form for the other two transitions is given in [*Xie and Tackley*, 2004a; 2004b]. The technical implementation of phase changes in STAG3D has been discussed in detail in [*Xie and Tackley*, 2004a; 2004b]. To summarize: a different reference state is calculated for each phase, and the properties in a particular grid cell (most importantly, reference density) depend on the relative fraction of the different phases as given by the appropriate phase functions. In order to avoid possible numerical problems associated with the last term in (2) when

Table 1. Default parameters.

Symbol	Meaning	Value
D	Mantle depth	2890 km
r_{cmb}	Core radius	3480 km
T_s	Temperature: surface	300 K
ρ_s	Density: surface	3300 kg.m^{-3}
ρ_{cmb}	Density: CMB	5600 kg.m^{-3}
α_s	Expansivity: surface	5×10^{-5} K^{-1}
α_{cmb}	Expansivity: CMB	1×10^{-5} K^{-1}
k_s	Conductivity: surface	3.0 W m^{-1} K^{-1}
k_{cmb}	Conductivity: CMB	6.54×10^{-5} m^{2}s^{-1}
g	gravity	9.8 m.s^{-2}
$\Delta\rho_{ppv}$	PPV density jump	66.4 kg m^{-3}
Di_s	Dissipation number: surface	1.18
<Di>	Dissipation number: depth-averaged	0.38
γ_s	Gruneisen parameter: surface	1.1
Cp	Specific heat capacity	1200 K kg^{-1} K^{-1}

Γ_i changes rapidly, the advection step is performed on potential temperature rather than total temperature, as potential temperature is not changed by phase transitions or adiabatic heating/cooling so has a much simpler energy equation. Potential temperature is then transformed to actual temperature to compute other terms in (2). This approach does not include the "effective heat capacity" discussed in [*Christensen and Yuen*, 1985]. To test whether this makes an important difference, the spherical axisymmetic cases in section 3.2 were recomputed using the phase change treatment in [*Christensen and Yuen*, 1985], i.e., with an effective thermal expansivity and effective heat capacity. The general behavior and the trends in internal temperature as a function of phase change parameters were found to be the same.

In presented cases where compositional variations are included, they are assumed to arise from melt-induced differentiation, which is treated in the same manner as in previous studies [*Nakagawa and Tackley*, 2004b, 2005a; 2005b; *Xie and Tackley*, 2004a; 2004b]. After each time step, the local temperature is compared to a depth-dependent solidus (shown in Plate 1 of [*Nakagawa and Tackley*, 2004b]). When the temperature in a cell exceeds the solidus, the fraction of melt necessary to bring the temperature back to the solidus is generated and instantaneously placed at the surface to form crust, then the cell temperature is set back to the solidus [*Xie and Tackley*, 2004a]. Composition is represented by the variable C, which varies from 0 (harzburgite) to 1 (MORB). In some cases the density contrast between these extremes is taken to be constant with depth for simplicity, but in later cases the multi-phase approach discussed in [*Xie and Tackley*, 2004a; 2004b] is used: the depth profile of density is calculated separately for pure olivine and pure pyroxene compositions, resulting in a depth-dependent density contrast between MORB and harzburgite. In the cases with compositional variations, radioactive heating is included and is enhanced by a factor of ten in the dense material to crudely account for the partitioning of incompatible heat-producing elements into the oceanic crust. Thus:

$$R_h(C,t) = H_0\left(\frac{1+9C}{1+9\langle C\rangle}\right)\exp((t_a - t)\ln 2/\tau) \qquad (3)$$

where H_0 is the present-day heating rate in the regular mantle, t_a is the age of the Earth (4.5 Gyr), t is the time since the beginning of the calculation and τ is the average half-life of radiogenic heating, taken to be 2.43 Gyr. The average present-day internal heating rate in the mantle is set to 23.7 in the non-dimensional equations, corresponding to a dimensional value of 6.2×10^{-12} W/kg.

The boundary conditions at the top and bottom boundaries are impermeable and shear stress free for velocity, isothermal for temperature and zero mass flux for composition. The side boundaries are periodic for all geometries except axisymmetric spherical, for which they are reflecting. The cases with melting-induced compositional variations have a time-dependent CMB temperature to account for cooling of the core, whereas other cases have a fixed CMB temperature. When core cooling is included, the bottom thermal boundary condition is given by $dT_{CMB}/dt = -KF_{CMB}$ where T_{CMB} is CMB temperature, which is initially set to 4200 K, K is the cooling coefficient given as $K = 3\rho_m c_m d/\rho_c c_c r_{CMB}$ (e.g., [*Steinbach, et al.*, 1993]), and F_{CMB} is the CMB heat flow given by the thermo-chemical mantle convection calculation.

Additional model details relevant to each study are given below.

3. THERMAL CONVECTION

This section discusses models that treat purely thermal convection, i.e., without compositional variations. The discussion starts with the study of [*Nakagawa and Tackley*, 2004a], performed in 2D cylindrical geometry, then progresses to new results in spherical geometry (axisymmetric or 3D spherical shell). All of these models include the compressible anelastic reference state with depth-dependent parameters described in section 2 (values given in Table 1), and a viscosity that is moderately temperature-dependent (by 3 orders of magnitude) and depth-dependent (2 orders of magnitude). All of these models are entirely heated from below, in order to emphasize the dynamics of the lower thermal boundary layer. They are thus not intended to be realistic Earth models, but rather give some theoretical guidance as to the influence of PPV on lower boundary layer dynamics.

3.1. Cylindrical Models

Plate 1 shows two-dimensional cylindrical models from [*Nakagawa and Tackley*, 2004a]. In these models, the post-perovskite transition was parameterized at a fixed depth of 2700 km, with the buoyancy due to phase change deflection included as mass anomalies at that depth and latent heat release or absorption also occurring at that depth, a method that has commonly been used to model the changes at 410 km and 660 km depth, e.g., [*Tackley, et al.*, 1993, 1994], which are also included in this model. These models had a reference Rayleigh number of 6×10^7, resulting in a time-averaged heat flow of 41-49 TW depending on the Clapeyron slope, which varied from 0 to +16 MPa K^{-1}, as given in Plate 1.

These results indicate that the post-perovskite transition has a small but noticeable effect on plume dynamics and mantle temperature. Whereas the case with zero Clapeyron slope has a fairly stable plume, positive Clapeyron slopes result in more time-dependent plumes and a slightly higher

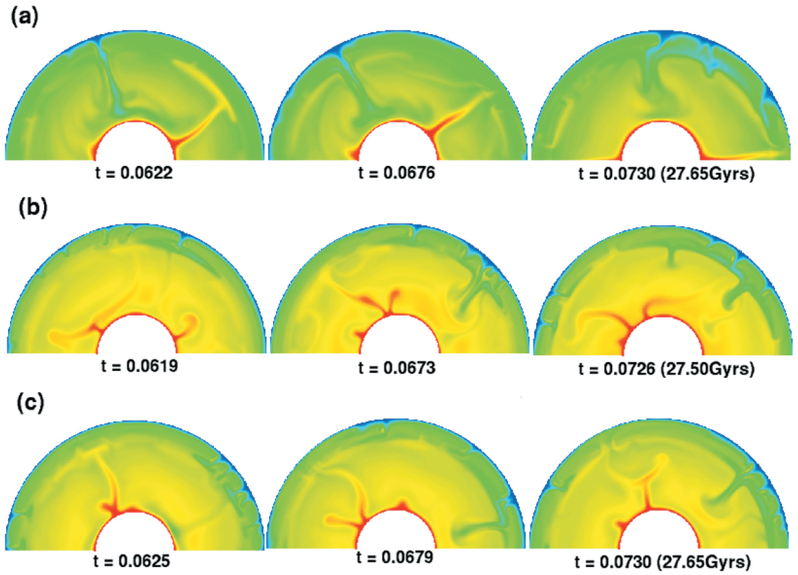

Plate 1. The time variation of the temperature field for three thermal convection cases with different Clapeyron slopes of the post-perovskite transition, from [*Nakagawa and Tackley*, 2004a]. Top row (a) has zero Clapeyron slope, middle row (b) has 8 MPa/K and bottom row (c) has 16 MPa/K. Red indicates high temperature and blue indicates low temperature.

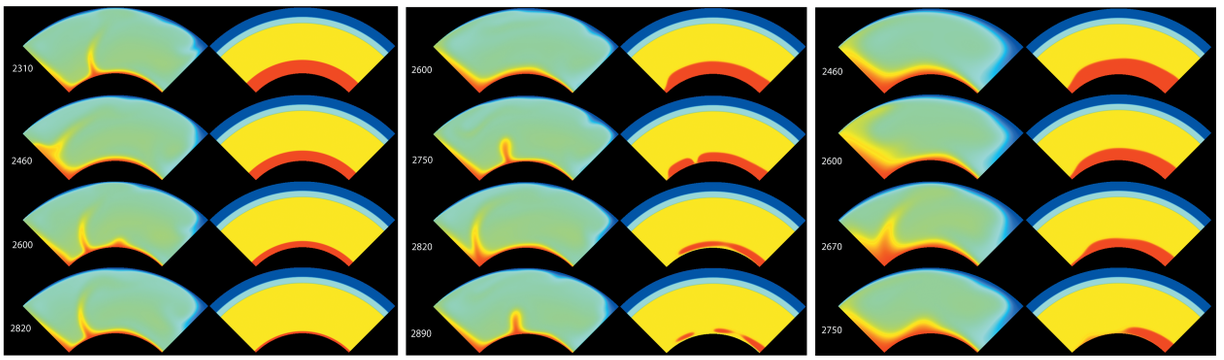

Plate 2. Spherical axisymmetric models with varying PPV phase change pressure and using the fixed depth approximation with $Ra_0=10^7$ (left panel), the phase function approximation with $Ra_0=10^7$ (center panel) or the phase function approximation with $Ra_0=10^6$ (right panels). The left column of each panel shows superadiabatic temperature (red=hot to blue=cold) whereas the right column of each panel shows phase function (red=postperovskite, yellow=perovskite, light blue=spinel, blue=olivine). The PPV phase change depth in km is written by each pair of plots.

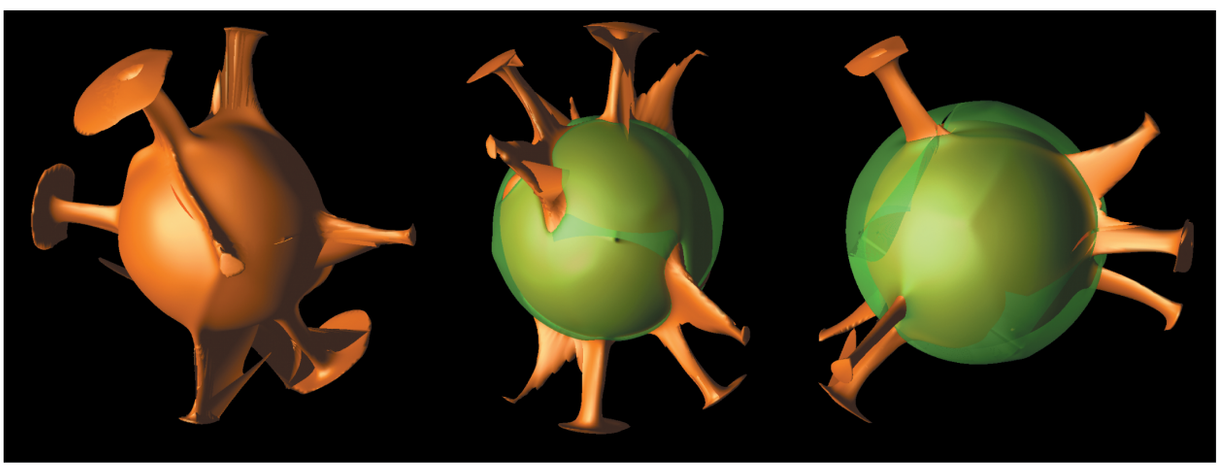

Plate 3. 3D spherical thermal convection: Isosurfaces of superadiabatic temperature (orange) and the PPV phase boundary (green) for three spherical cases with (left) zero PPV Clapeyron slope, (middle) the default Clapeyron slope and phase boundary 72 km above the CMB ($d_{ppv}=0.975$), (right) the default Clapeyron slope and phase boundary 289 km above the CMB ($d_{ppv}=0.9$).

mantle temperature. This suggests that the net effect of the post-perovskite transition is to destabilize the lower thermal boundary layer, consistent with the results of [*Matyska and Yuen*, 2005] and earlier findings on the effect of the exothermic phase change that causes the 410 km discontinuity. It is also consistent with previous convection models of Mars in which a phase transition of the opposite sign, i.e., the endothermic γ-spinel to perovskite+magnesiowüstite transition, was placed close to the CMB, both in 2D cylindrical [*Weinstein*, 1995] and 3D spherical shell [*Harder*, 1998; *Harder and Christensen*, 1996] geometries. In those models, the phase transition had the opposite effect, i.e., to generate fewer, stronger plumes. These Mars calculations used the Boussinesq approximation, in which latent heat is ignored, and thus the only phase change effect is buoyancy due to phase change deflection, which for an exothermic transition like PPV clearly enhances convection. In compressible models latent heat must be included, which for an exothermic phase transition acts to stabilize convection [*Schubert and Turcotte*, 1971; *Schubert, et al.*, 1975] because it reduces the temperature of upwellings. For Mars, [*Zhou, et al.*, 1995] and [*Breuer, et al.*, 1996] appeared to find that the latent heat effect of the exothermic olivine to spinel transition may be important. However, latent heat seems unlikely to be important for the PPV transition, because the latent heat for PPV corresponds to only a 40-50 K temperature change, which is more than an order of magnitude less than the temperature drop over the lower thermal boundary layer in Earth's mantle (~1000-1500 K) and the superadiabatic temperature variations driving thermal convection (up to 2500 K). Only if latent heat is exaggerated by a factor of 10 does it have a measurable effect [*Kameyama and Yuen*, 2006]. Therefore it is not surprising that in these results the net effect of PPV is destabilizing.

These models have several shortcomings. One is that the large vertical deflection of the PPV boundary and the possibility of a double crossing imply that approximating the transition at a fixed depth may be a poor approximation, and its deflection should instead be treated with a phase function approach as detailed in section 2. Another shortcoming is the geometry: the real Earth is spherical and 3D. Additionally, there is some uncertainty in the phase change pressure (depth), so it would be useful to know what effect this has. These aspects are addressed now with new models.

3.2. Spherical Axisymmetric Models

In order to test the effect of the PPV transition and its numerical treatment on mantle temperature, a systematic suite of simulations in axisymmetric spherical geometry has been performed. The model spans a hemisphere from the pole to the equator. The parameters are similar to those in [*Nakagawa and Tackley*, 2004a], i.e., heated from below with mildly temperature- and depth-dependent viscosity, except that the reference Rayleigh number is a factor of 6 lower (1×10^7 instead of 6×10^7), which is best interpreted to mean that the reference viscosity is 6 times higher, and the phase transitions at 410 and 660 km depth are not included. The CMB temperature is fixed at 3600 K, and the numerical grid has 128×64 cells. Cases were initialized in such a way that a plume formed at the axis (pole), and run until they reached secular equilibrium. Two sets of runs were performed: one with a fixed-depth transition and one with the phase function approach. The PPV phase transition depth was systematically varied. For the fixed-depth approximation this is the actual depth, whereas for the phase function approximation it means d_{ppv} in equation (1), with T_{ppv} set to 3000 K and γ_{ppv} set to +12 MPa K^{-1} (a rather high value in order that the effect of the PPV transition is clear); therefore in low temperature regions PPV can exist even with d_{ppv} set to at or below the CMB. In general the actual PPV transition depth is shallower than d_{ppv}. Additionally, the second set of runs was repeated with a reference Rayleigh number an order of magnitude lower i.e., 10^6, in order to test the effect of thermal boundary layer thickness.

Plots of superadiabatic temperature and phase function (Plate 2) show an upwelling plume at the axis of symmetry (left side) and a downwelling sheet at the equator (right side). Time-dependent instabilities form from the lower boundary layer and are swept into the main plume. The post-perovskite transition appears to have a rather small effect on the temperature structure; the main difference in the appearance of the different parts of Plate 2 is due to time-dependent instabilities. The center panel shows the change in the appearance of the post-perovskite region as the phase transition pressure is increased from a global, strongly-undulating layer to a double-crossing and isolated patches. At lower Rayleigh number (right panel) the boundary layer is thicker.

Despite this apparently small effect on the dynamics, there is a notable effect on volume-averaged mean mantle temperature, as show in Figure 1, with a difference of as much as 125 K. The maximum effect is independent of phase change numerical treatment, but the mean temperature is much more sensitive to phase change pressure in the more realistic phase function approach than it is with the fixed-depth parameterization. With a fixed-depth parameterization, the effect is maximum when the transition occurs above the bottom thermal boundary layer. With the more realistic phase function approach and $\mathrm{Ra}_0=10^7$, the effect is maximum when there is a double crossing and the PPV covers most of the CMB (the 2820 km case) but diminished when PPV becomes more patchy, or forms a thick layer with a single crossing. At an order of magnitude lower Rayleigh number the peak is shifted to a greater distance from the CMB, implying that it

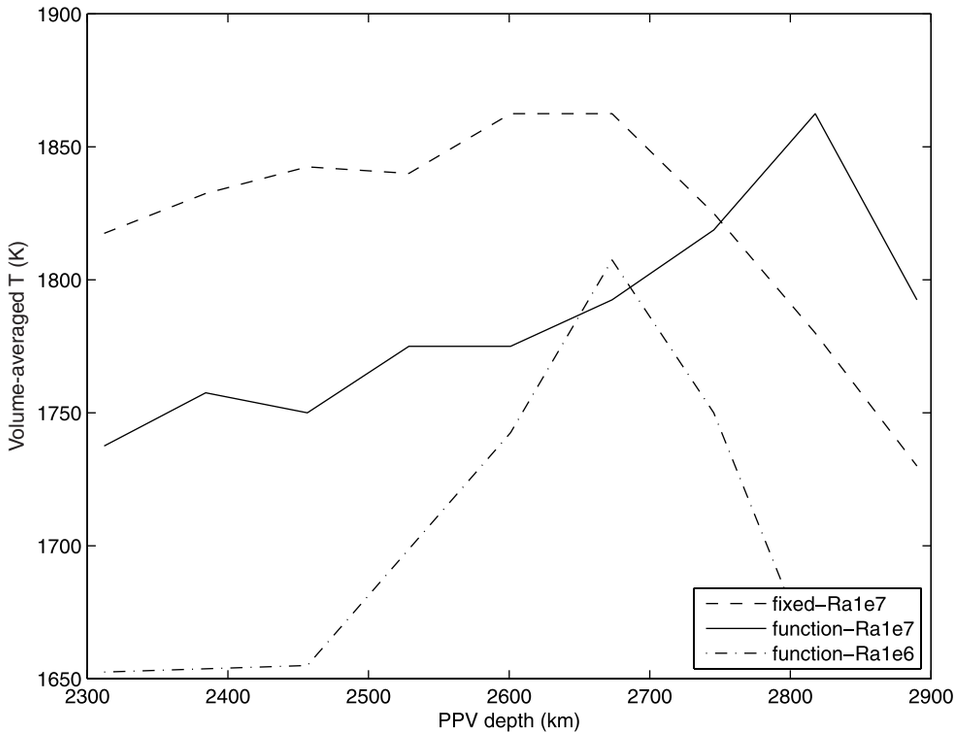

Figure 1. Mean mantle temperature as a function of PPV phase change depth for axisymmetric spherical models using either the fixed depth approximation (blue) or phase function approximation (green and red). The blue and green lines are for cases at $Ra_0=10^7$ whereas the red line is for $Ra_0=10^6$.

is the ratio of PPV layer thickness to thermal boundary layer thickness that is important. This dependence on phase change depth and thermal boundary layer thickness may explain why different studies apparently find different effects on mantle temperature.

3.3. 3D Spherical Models

3D spherical results were computed for three of the above cases- the ones with zero Clapeyron slope, with phase function pressure=2820 km, and with phase function pressure=2600 km. The case with zero Clapeyron slope was run to statistical equilibrium, then the other cases were started using this case as an initial condition and run until the mean temperature stabilized. A resolution of 64×192×64×2 was generally used, i.e., 64 radial points and a horizontal grid spacing equivalent to having 256 cells around the equator, but after reaching equilibrium the cases were continued for about 10,000 time steps at double this resolution, i.e., 128×384×128×2, to check that there is no significant change in behavior or mean temperature.

Plate 3 shows upwelling plumes and the location of PPV for these cases. In the reference case, about 7 plumes are visible, fairly evenly spaced around the domain. In the case with d_{ppv}=2820 km, for which in axisymmetric geometry PPV was found to display the largest effect, the planform is significantly different, with two major plume groups in opposing hemispheres and about 9 plumes in total. The case with the deep PPV layer (d_{ppv}=2600 km) is more similar to the reference case, with four plume clusters in a roughly tetrahedral configuration, and about 9 plumes in total. While it is tempting to conclude from these results that in 3-D the post-perovskite transition favors the formation of plume clusters rather than isolated plumes, more research needs to be done to verify this. The volume-averaged mean temperature for these cases is 1712 K, 1835 K and 1775 K respectively, which is similar to the axisymmetric cases. Temperature profiles for these cases are shown in Figure 2. Interior temperature profiles are approximately parallel, but offset from each other.

4. THERMO-CHEMICAL CONVECTION

Several lines of evidence point to compositional variations being very important in the mantle, as discussed earlier, and it is therefore important to study the interaction of compositional variations with the post-perovskite phase transition.

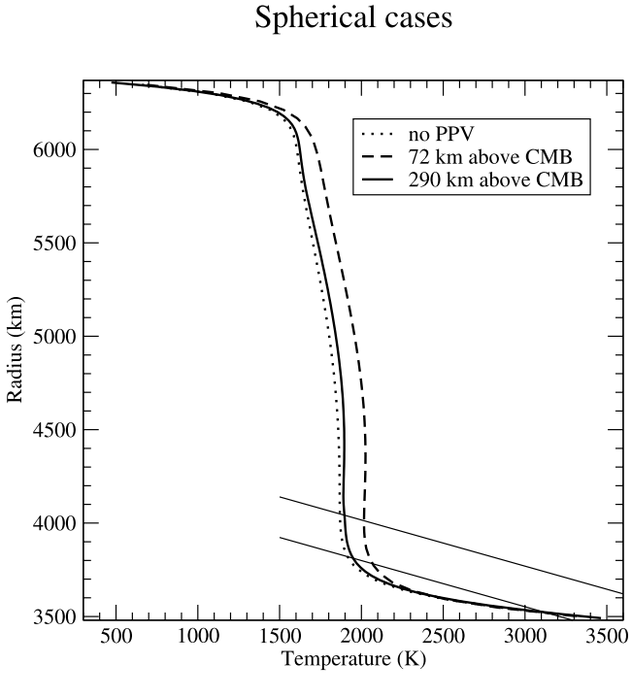

Figure 2. Temperature profiles (geotherms) for the 3D spherical cases shown in the previous Figure. The two different assumed positions of the phase boundary Clapeyron slope are also indicated (light solid lines).

4.1. Two-Dimensional

In the 2D cylindrical study of [*Nakagawa and Tackley*, 2005b] (Plate 4), compositional variations arose through partial melting-induced differentiation of the mantle from a homogeneous start, with secular cooling of the core and the decay of radiogenic heat-producing elements accounted for. The models also included much stronger temperature-dependence of viscosity and plastic yielding to mobilize the lithosphere. For full model details the reader is referred to [*Nakagawa and Tackley*, 2005b]. The density difference between subducted MORB and harzburgite, which is rather uncertain from mineral physics constraints, was set to either 0, 2% or 3% of the reference (surface) density, i.e., 0, 66 or 99 kg m^{-3}, and the PPV transition Clapeyron slope was set to either 0, 8 MPa/K ("predicted") or 16 MPa/K ("exaggerated"). The time-evolution of a typical case over billions of years is plotted in the top panel of Plate 4. Early on, vigorous upper mantle convection results in a depleted upper mantle, but subsequent whole-mantle stirring leads to compositional heterogeneity everywhere, sometimes with some accumulation of dense subducted crust above the CMB. Of particular interest here is the evolution of the post-perovskite field, which is shown in the center column. This shows clearly the transition from isolated patches of PPV and a double-crossing, to a continuous but strongly-undulating layer, as the core and mantle cool.

In this study, PPV has a significant influence on the stability of dense material at the CMB, as shown in the lower panel of Plate 4, which compares final states for three different values of the Clapeyron slope. With a zero Clapeyron slope, dense crust can accumulate at the CMB, although at this density contrast the layer is quite messy. With the 'predicted' Clapeyron slope, dense material is less stable at the CMB and instead large 'piles' are formed, stretching at least half way across the mantle. The tops of these piles are not sharp, although their sides can be. Finally, if the Clapeyron slope is set to an exaggerated value, it is difficult for coherent accumulations of material to form at all above the CMB.

In cases where MORB forms piles at the CMB, there is an anticorrelation between these piles and the occurrence or thickness of a PPV layer. This is because the piles are hot, so the geotherm either misses the PPV boundary (if the CMB temperature is in the perovskite temperature field) or rapidly crosses into the perovskite stability field (if the CMB temperature is in the PPV stability field). This does not take into account the composition-dependence of the post-perovskite boundary, as further discussed later.

4.2. Three-Dimensional Cartesian

This type of model was extended to 3D Cartesian geometry by [*Nakagawa and Tackley*, 2006], again considering a range of compositional density contrasts. Plate 5 shows isosurfaces of temperature, composition and PPV fields for four different compositional density contrasts ranging from 0 to 2% of the reference (surface) density. Again, when the crust is dense there is a tendency to form a 'messy' layer above the CMB. In these calculations, the final CMB temperature arises from 4.5 billion years of secular evolution, and is thus strongly influenced by composition: in the cases with a higher density contrast, dense material accumulating above the CMB reduces the core heat flux resulting in a hotter final core, so that PPV is still in the double-crossing, isolated patch regime.

In order to compare numerical models to seismological observations it is important to calculate the seismic velocity field that arises from given variations in temperature, composition and phase. In the deepest mantle, the seismic S-wave velocity jump over the PPV transition is comparable to Vs variations arising from temperature or composition, so lateral variations in the occurrence of PPV can have a major or dominant effect on long-wavelength lateral seismic heterogeneity. [*Nakagawa and Tackley*, 2006] plotted the lateral seismic power spectra of Vs at 2700 km depth for the four different density contrasts using scaling factors for temperature and composition from [*Trampert, et al.*, 2004], and found that lateral variations in the occurrence of PPV are the

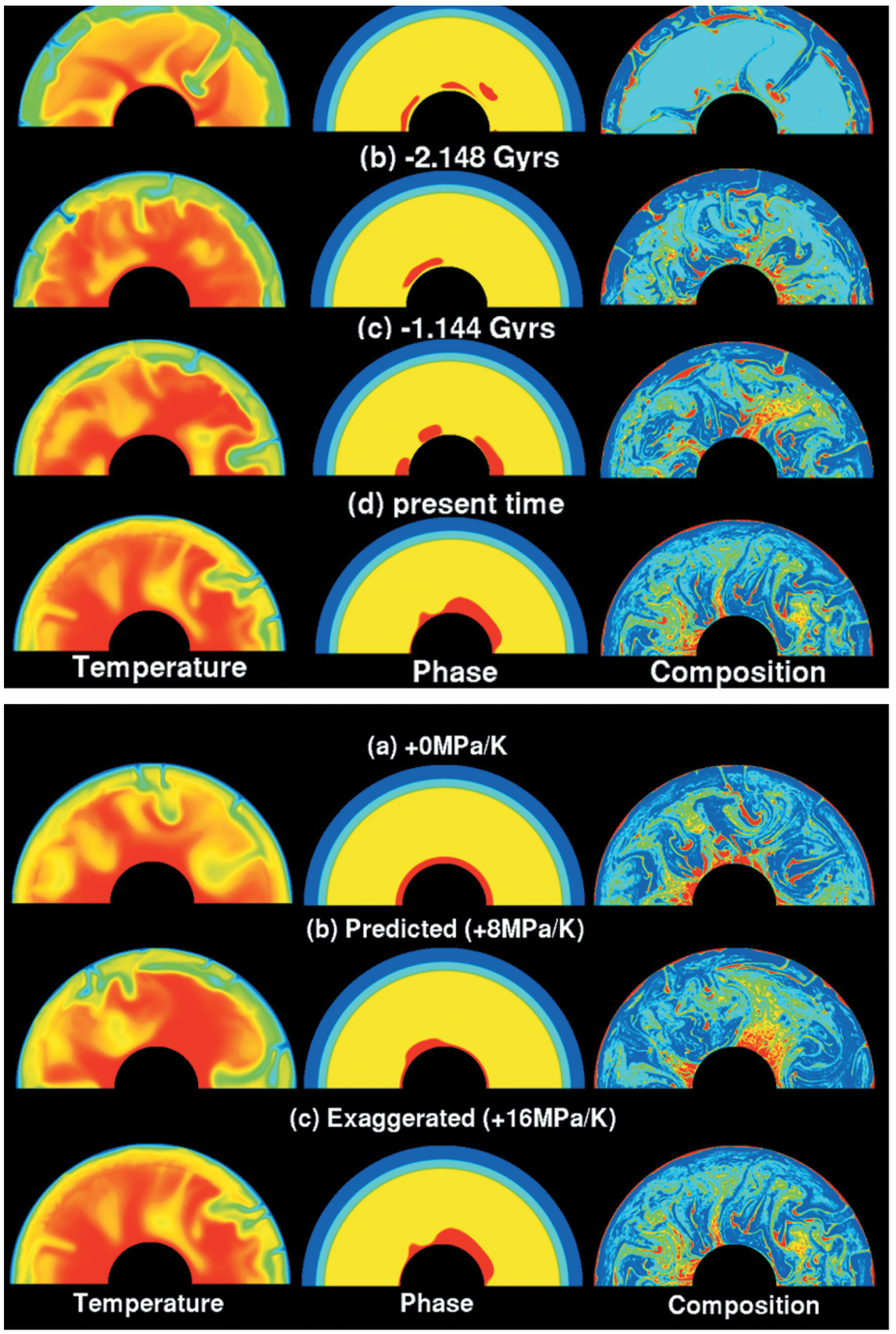

Plate 4. Thermo-chemical convection models including the PPV phase transition, reproduced from [*Nakagawa and Tackley*, 2005b] with permission. Top Panel: The time evolution of (left) temperature, (center) phase function, and (right) composition for a case with an exaggerated PPV Clapeyron slope. The composition varies from MORB (red) to harzburgite (blue), and the temperature and phase function scales are as in Plate 2. Each row represents a different time before present, as indicated. Bottom Panel: Temperature, phase function and composition fields for cases with a 2% compositional density contrast and three different Clapeyron slopes.

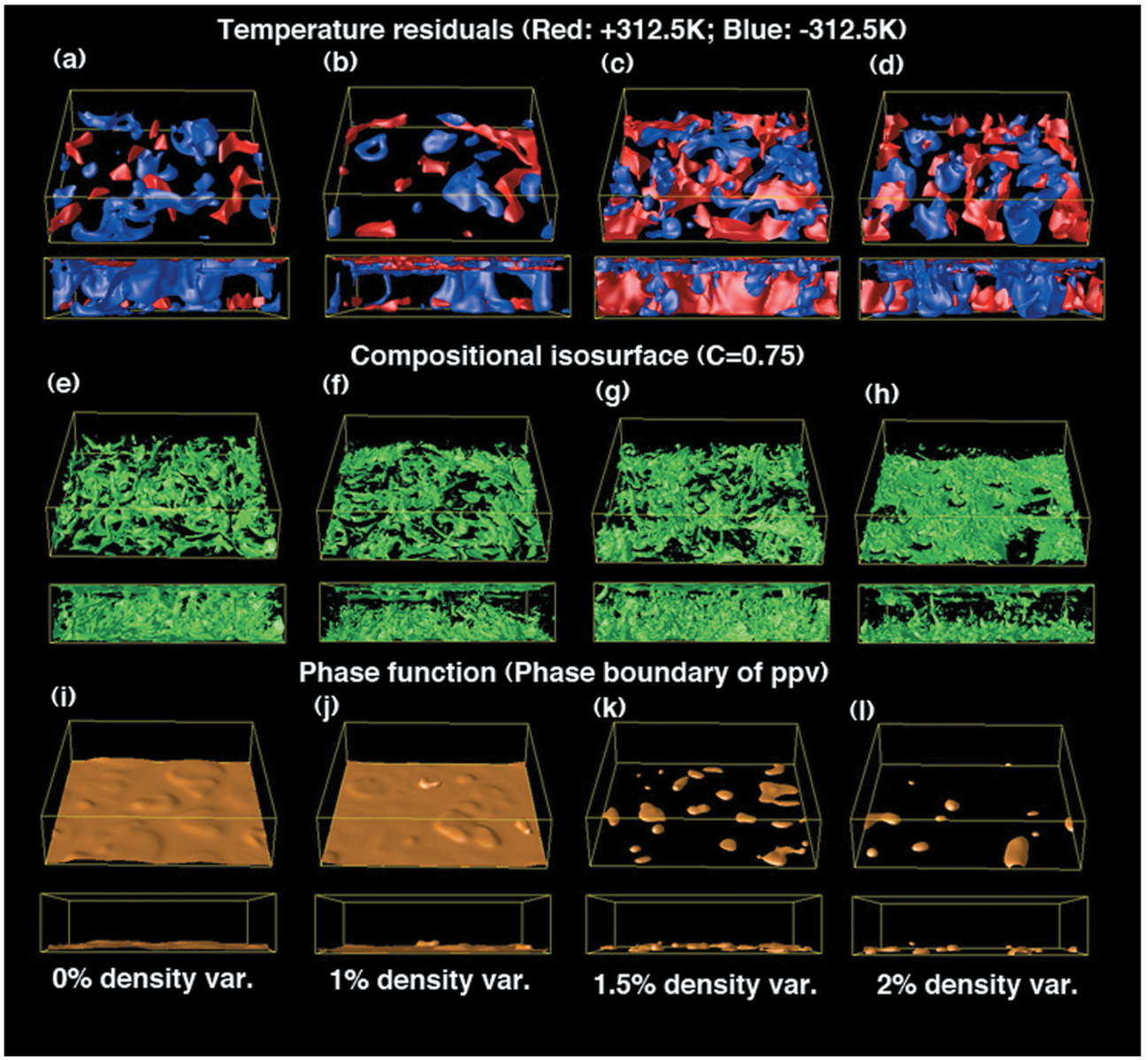

Plate 5. Isocontours of residual temperature, composition, and phase function, for 3D Cartesian models with different compositional density contrasts, reproduced from [*Nakagawa and Tackley*, 2006]. The temperature isocontours show where the temperature is 312.5 K higher (red) or lower (blue) than the horizontal average. The compositional isosurfaces show C=0.75, i.e., >75% MORB. The phase function plots show the location of the post-perovskite phase.

dominant contributor to long-wavelength seismic heterogeneity at this depth. As previously found [*Nakagawa and Tackley*, 2005b], composition has a relatively "flat" spectrum whereas temperature has a "red" spectrum, so that composition becomes the dominant at shorter wavelengths. The contribution of PPV has a spectral slope that is intermediate between those of temperature and composition.

Here, for additional information, we plot spectra for the whole mantle in the form of spectral heterogeneity maps [*Tackley, et al.*, 1994]. Plate 6 shows SHMs for the four cases in Plate 5. These confirm that the temperature spectra are quite "red" while the compositional spectra are broader, i.e., extend to higher spatial frequencies. Near the CMB, the contribution of PPV to long-wavelength lateral heterogeneity is larger than the contributions of composition or temperature. Composition can be similarly important to temperature, particularly at the top (where the crust and lithosphere exist) and in the lower ~1/3 of the mantle, where compositionally-distinct material accumulates or spreads out. In [*Tackley*, 2002] it was demonstrated that a thick undulating layer of dense material generates a large contribution to Vs at mid lower mantle depths because of the thermal boundary layer at the top of the layer. The "layers" that form in the present calculations, in contrast, do not have sharp tops with a well-defined sharp boundary, so this consideration does not apply.

4.3. 3-D Spherical With Composition-Dependent PPV Depth

These investigations are currently being extended to 3D spherical geometry with composition-dependent PPV phase change depth. Plate 7 shows two preliminary results, again after billions of years of evolution. The physical parameters are similar to those in [*Nakagawa and Tackley*, 2005b] with a PPV Clapeyron slope of 8 MPa/K and an initial CMB temperature of 4300 K, except that the treatment of chemical density variations is different: whereas [*Nakagawa and Tackley*, 2005b] assumed a chemical density contrast that is constant with depth, these calculations use different reference states for the pyroxene-garnet and olivine systems as in [*Nakagawa and Tackley*, 2005a; *Xie and Tackley*, 2004a; 2004b], which allows each system to have different depths for the various phase changes as well as different compressibilities. The density contrast between olivine and pyroxene components at the CMB pressure is 1.8%, corresponding to the "intermediate" case in [*Nakagawa and Tackley*, 2005a]. In the case with different PPV transition depths, the pyroxene component (of which MORB is mostly comprised) undergoes the transition 150 km shallower than the olivine component (of which harzburgite is mostly comprised). This difference corresponds to about 8 GPa, consistent with recent mineral physics results (K. Hirose, personal communication, 2007).

In both of these spherical cases the flow pattern has a very long-wavelength nature, and a "messy" layer of subducted MORB forms, which is swept aside in regions where downwellings reach the CMB region. A major difference is observed in the location of the PPV phase. When the transition depth is independent of composition, PPV is only found in isolated patches in cold regions where subducted slabs pool, as in the 2D cylindrical and 3D Cartesian results discussed above. However, when PPV occurs at lower pressure in MORB-rich regions, then PPV is found everywhere above the CMB. Indeed, the higher temperature of the 'piles' of MORB is more than compensated for by the shallower pressure of the phase boundary, so that PPV occurs at shallower depth in hot MORB piles.

The use of spherical geometry facilitates the calculation of lateral spectra directly in spherical harmonics, and these are shown in Plate 8. They look broadly similar to those for the Cartesian cases (Plate 6), and also similar to each other, showing that geometry and composition-dependence of PPV transition depth do not have a first-order effect on long-wavelength lateral heterogeneity, although the regional structures can look quite different (Plate 7).

5. CONCLUSIONS AND DISCUSSION

5.1. Findings From Numerical Calculations

From the numerical modeling discussed above, various conclusions can be drawn.

(1) The dynamical effect of the PPV transition is small but measurable.
(2) The PPV transition slightly destabilizes the lower boundary layer. If a purely thermal boundary layer, this will influence the manifestation of upwelling plumes. If thermo-chemical, it reduces the stability of dense material at the CMB, such that a larger chemical density contrast is required to stabilize 'piles'.
(3) The PPV transition slightly increases mantle temperature. The magnitude of the effect depends on the depth (pressure) of the transition relative to the thermal boundary layer thickness. A fixed-depth parameterization of the transition typically over-estimates this effect.
(4) Similar results are obtained in different geometries, including 2D cylindrical or axisymmetric spherical, or 3D Cartesian or spherical-shell.
(5) Lateral variations in the occurrence of PPV are the dominant contributor to long-wavelength lateral heterogeneity in the seismic shear wave velocity in the deepest mantle.
(6) The different contributions to seismic heterogeneity have different spectral slopes: temperature has a "red"

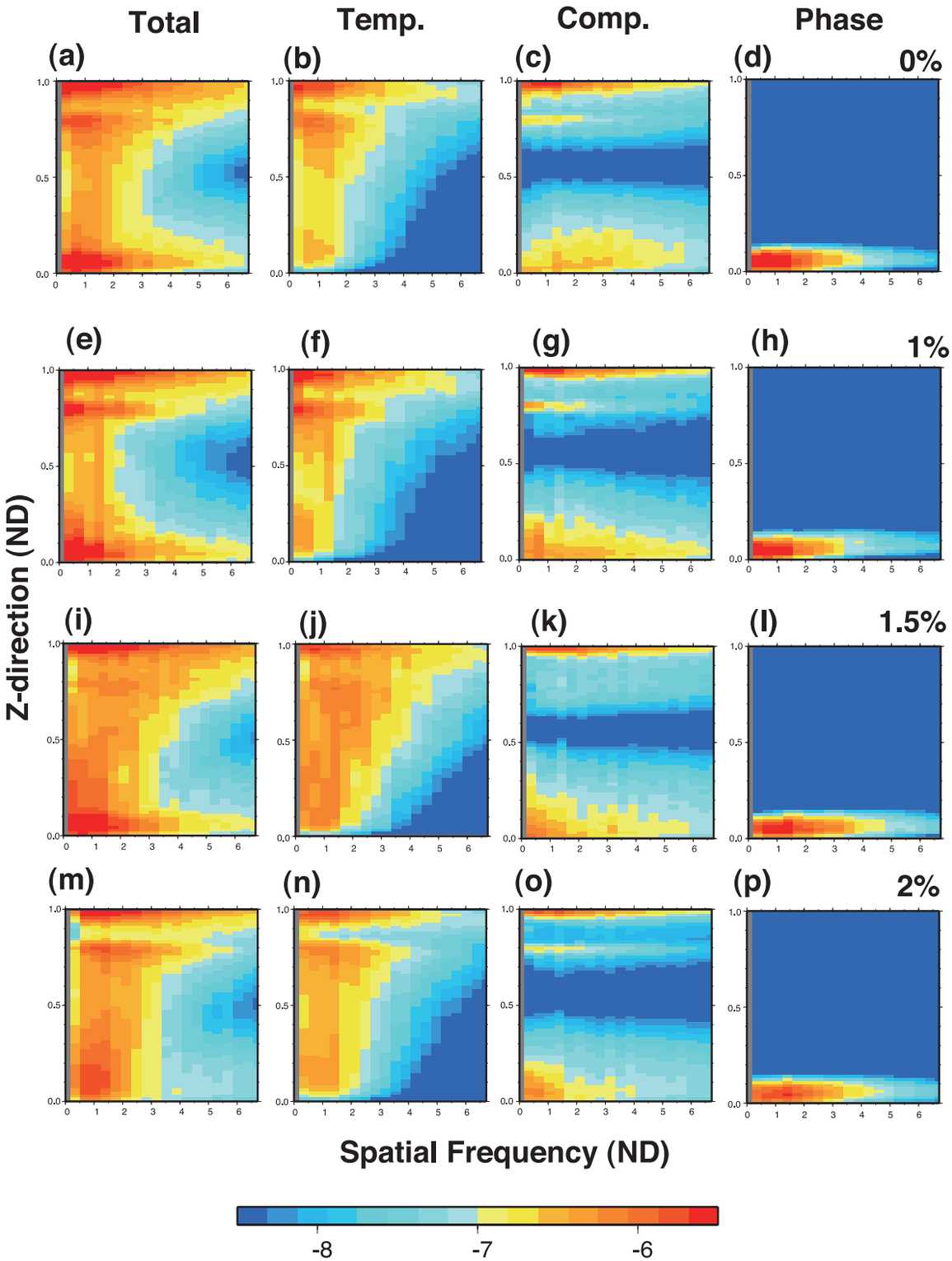

Plate 6. Spectral Heterogeneity Maps of seismic shear wave velocity for the 3D Cartesian cases in Plate 5. Plots show the power in the lateral heterogeneity spectrum as a function of vertical coordinate, from the CMB to the surface. (a)-(d) case with no chemical density contrast, (e)-(h) case with 1% chemical density contrast, (i)-(l) case with 1.5% chemical density contrast, (m)-(p) case with 2% chemical density contrast.

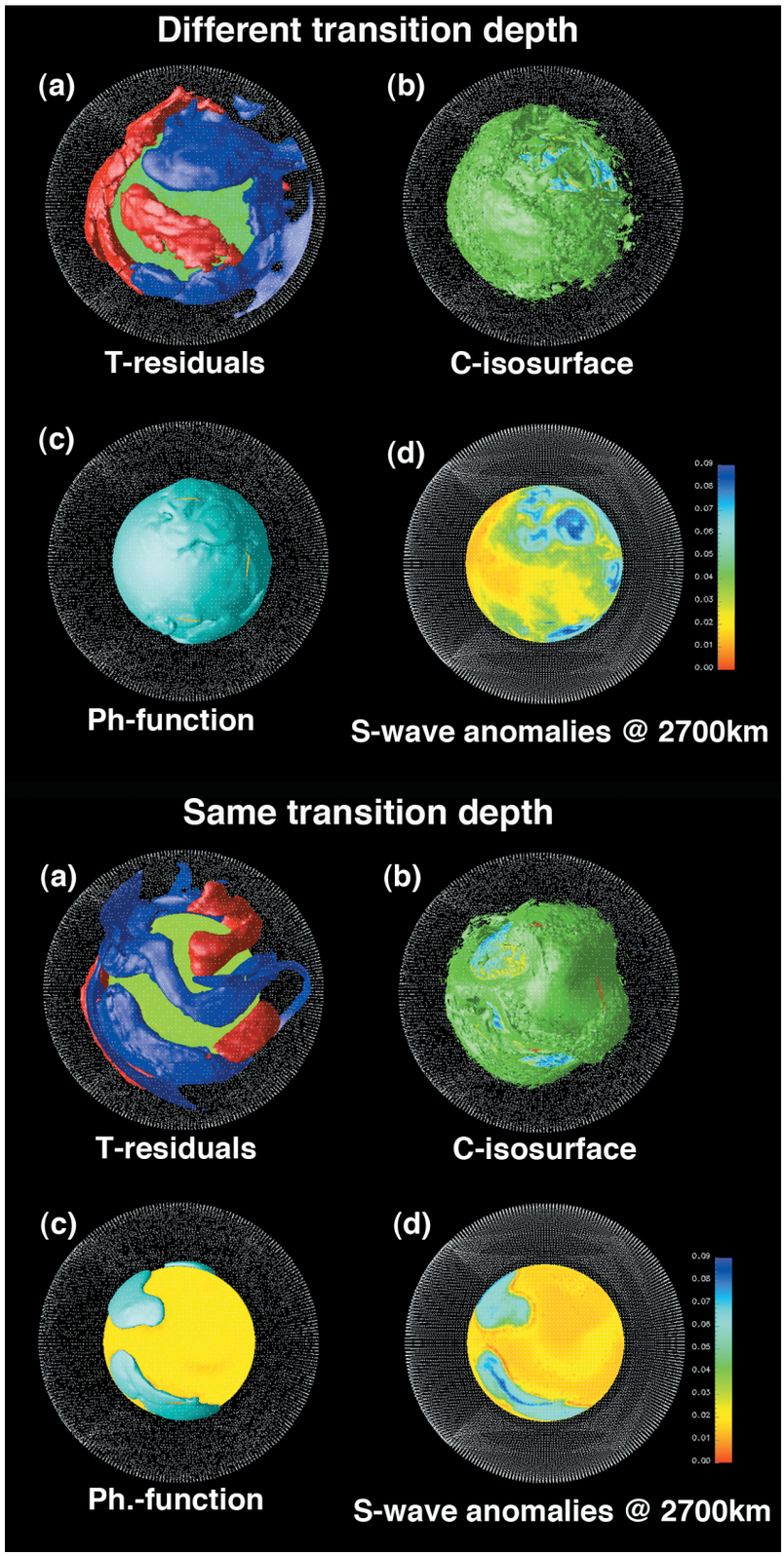

Plate 7. Thermo-chemical convection cases in 3D spherical geometry, showing the effects of composition-dependent PPV phase transition depth (top panel) compared to a case with composition-independent PPV depth (bottom panel). The parameters are otherwise similar to 2D cylindrical cases in Plates 4-5 and [*Nakagawa and Tackley*, 2005b], as discussed in the text. In each panel the plots are: (a) Residual temperature isosurfaces showing where the temperature is 250 K higher (red) or 250 K lower (blue) than the geotherm, with the upper 400 km removed to expose the deep mantle. (b) Compositional isosurface showing C=0.75, i.e., 75% "MORB" and 25% "harzburgite", again with the upper 400 km removed. (c) Location of at least 50% volume fraction post-perovskite. (d) S-wave anomalies at 2700 km depth, where Vs varies by 2% both for composition and with PPV.

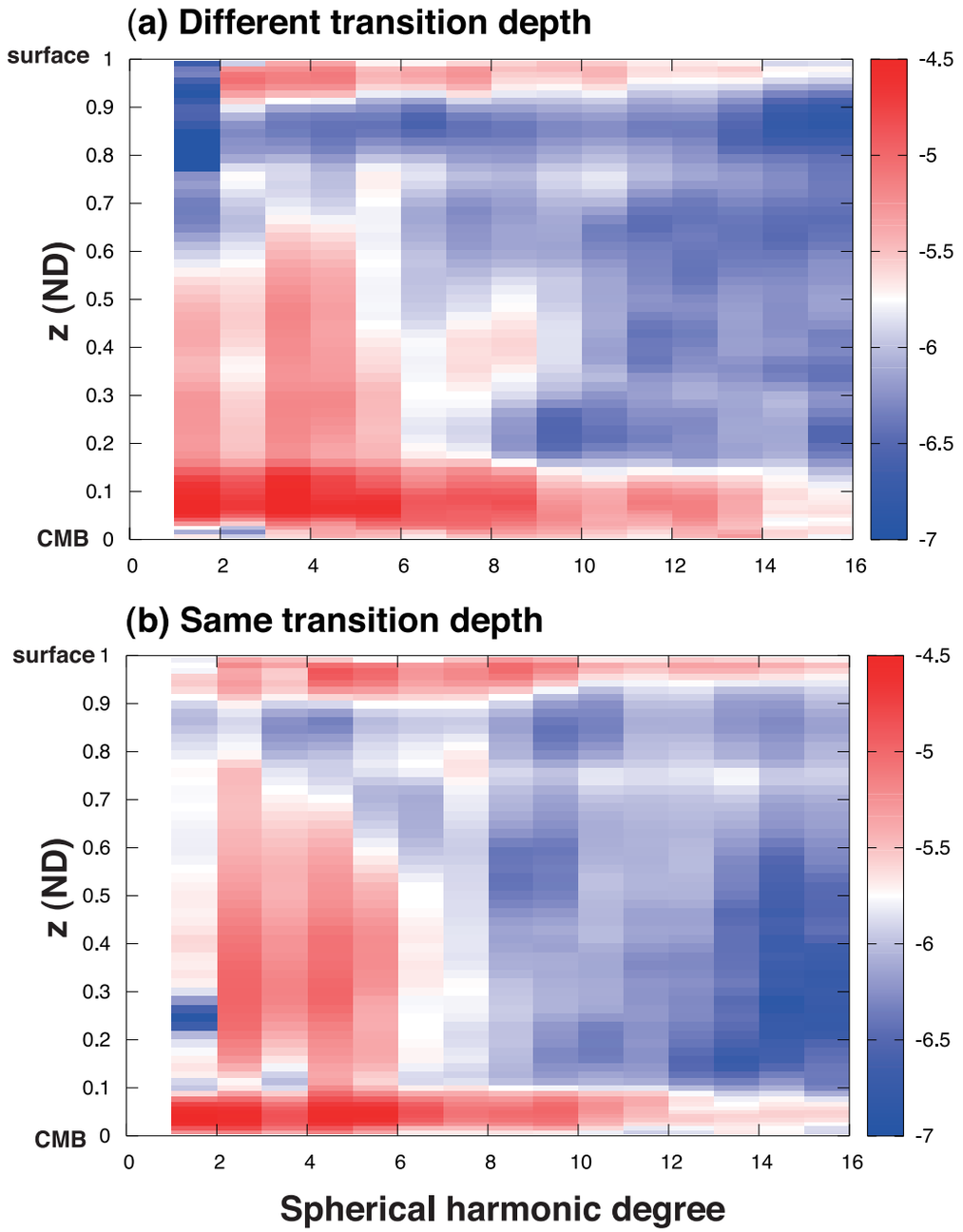

Plate 8. Spectral heterogeneity maps of seismic shear wave velocity for the two spherical cases in Plate 7, i.e., with or without composition-dependent PPV depth, again on a logarithmic scale. These show the combined effects of temperature, composition and phase on shear-wave velocity.

lateral temperature spectrum that decreases rapidly with increasing degree, the spectrum of composition is relatively flat (guaranteeing that composition is the dominant contributor to seismic wave velocity at short wavelengths) while the contribution of PPV variations is inbetween these slopes.

The following results can be deduced from simple considerations (i.e., consideration of geotherm relative to the phase boundary) but are reinforced by the numerical calculations.

(7) A zero-, single- or double- crossing of the PPV phase boundary can occur depending on the temperatures of the CMB and deep mantle.

(8) Regions where a thick PPV layer exists are anticorrelated with piles of dense material if the PPV boundary is not composition-dependent, because the vertical temperature profile through the hot dense piles may not intersect the PPV stability field at all (if the CMB is in the perovskite stability field) or crosses it very close to the CMB (if the CMB is in the PPV stability field).

(9) If a stable dense layer covers the entire CMB, then the transition to PPV may not occur at all (if the CMB is in the perovskite stability field) or occurs very close to the CMB (if the CMB is in the PPV stability field).

(10) A thick post-perovskite layer is typically found in regions where subducted slabs pool above the CMB, and sometimes isolated patches of post-perovskite are found in the tips of downwelling slabs as they approach the CMB region.

The "realism" of the numerical models could be improved in several ways, some of which are now discussed. Firstly, recent seismological investigations find features consistent with double-crossing of the PPV phase boundary [*Hernlund, et al.*, 2005; *Lay, et al.*, 2006; *Thomas, et al.*, 2004a; *Thomas, et al.*, 2004b; *van der Hilst, et al.*, 2007], which implies that the CMB is in the perovskite stability field, whereas in some of the presented cases it is in the PPV stability field. Secondly, the composition-dependence of the PPV should be taken into account [*Lay, et al.*, 2006; *Mao, et al.*, 2004; *Ono, et al.*, 2005; *Stackhouse, et al.*, 2006], as is further discussed in the next section. Thirdly, the calculation of Vs from temperature, composition and phase involves scaling coefficients that have a significant uncertainty, and may also be quite anisotropic [*Stackhouse, et al.*, 2006]. Fourthly, calculations could be closer to Earth-like in terms of convective vigor, temperature-dependence of viscosity, temperature-dependence of other material properties, and so on. Finally, small-lengthscale variations in composition and possibly the dynamics exist, which will require very fine resolution.

5.2. More Complex Scenarios

The double-crossing model envisioned by [*Hernlund, et al.*, 2005] was posited in the absence of information regarding potential compositional effects on the stability of PPV, and with the exception of the new results described above, dynamical models at the present time have yet to consider this effect. If PPV stability were modulated only by variations in temperature, then the earlier modeling results indicating absence of PPV in "piles" could present a paradox since one of the most definitive seismic detections of a feature resembling a PPV-lens occurs beneath the central Pacific [*Lay, et al.*, 2006] within the large low shear velocity province, which is presumably warmer than average D" mantle. Seismic detections of a discontinuity at similar depths in both seismically fast and slow regions suggests that, if due to PPV, some degree of chemical as well as thermal modulation of the phase boundary exists. Here we briefly discuss some of the issues this presents, some of the present uncertainties that impede a straightforward investigation of chemical variations, and why several possibly important dynamical effects depend on the nature of thermo-chemical modulation of PPV.

Figure 3 is meant to be illustrative only, and shows some of the potential variety of complex behavior that can occur when we consider chemical as well as thermal modulation of the appearance of PPV-bearing rock. In both panels, we suppose there may be a variety of chemically distinct patches within the deep mantle, with an uncertain relationship between one another. One example is the necessary fine layering of a subducted slab which has been segregated into MORB crust and a Harzburgite residuum, both of which should generally have a composition distinct from one another as well as from the surrounding average mantle, the latter of which itself may be heterogeneous at a variety of scales (though this is not shown in the figure). If large modestly dense chemically distinct material comprises the low shear velocity provinces beneath Africa and the Pacific, the behavior of the PPV transition may be different depending upon whether one is inside or outside these "piles." Finally, the fine layering at the base of the mantle responsible for ultralow-velocity zones, or ULVZ, may also be chemically distinct, particularly if recent seismic arguments for a ~10% density increase in ULVZ are robust [*Rost, et al.*, 2005]. Also shown are the relative temperature variations, labeled simply in terms of which settings we expect to be hot, warm, or cold. The coldest possible regions are necessarily associated with any subducted oceanic lithosphere and provide an important reference point for the most shallowly displaced discontinuities in seismically fast regions [*Hernlund and Labrosse*, 2007]. The edges of piles are expected to be hot due to the necessary counter-circulation inside the piles, which has

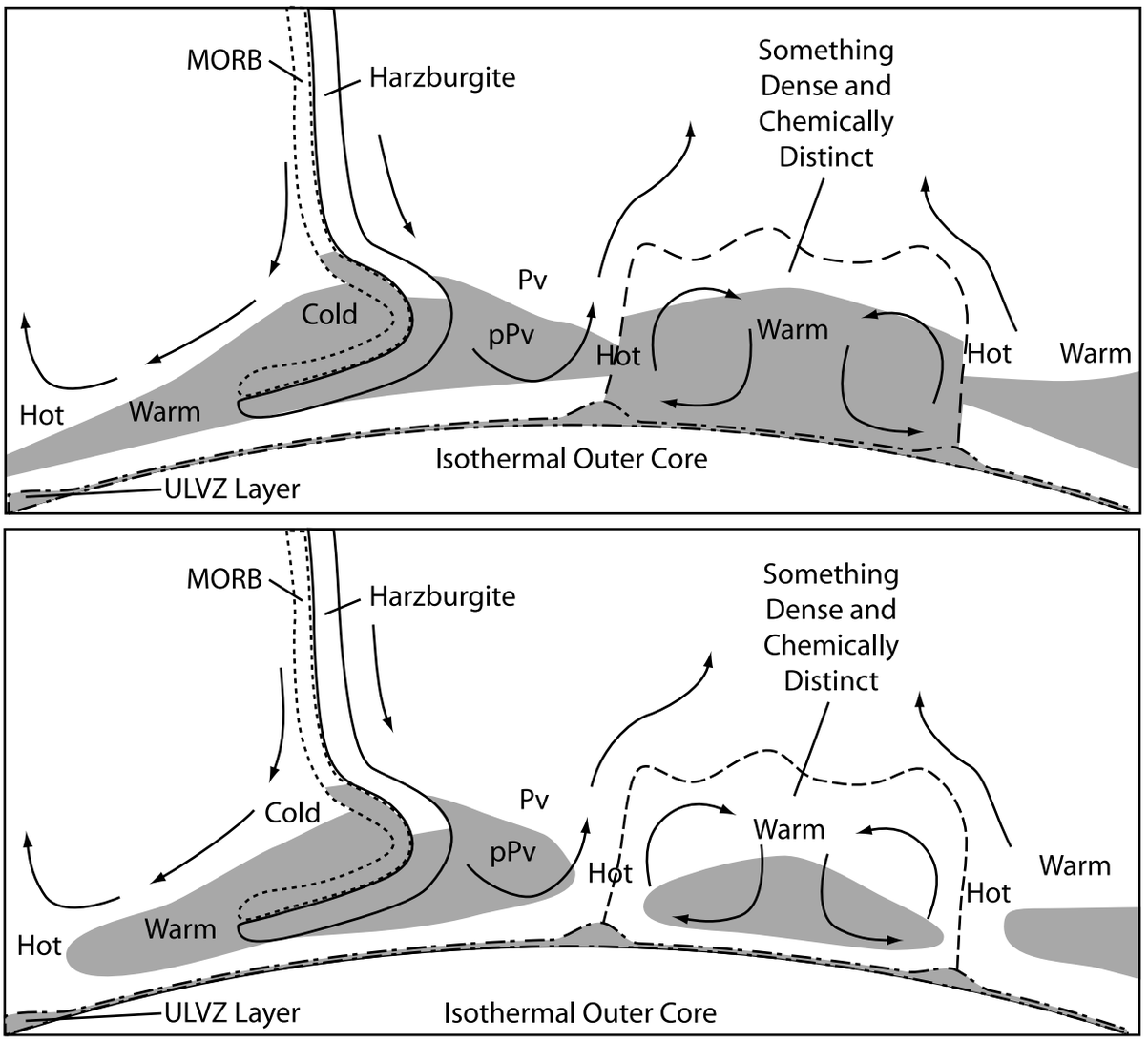

Figure 3. Cartoons of possible deep mantle structures arising from composition-dependent PPV transition. The lower panel is most similar to the scenario favored by the latest seismic observations of PPV lenses [*Lay, et al.*, 2006; *van der Hilst, et al.*, 2007]. See text for a detailed explanation and discussion of these scenarios.

been discussed in greater detail elsewhere (e.g., [*Lay, et al.*, 2006]). The interiors of piles will never be as cold as subducted slabs, since the material sits on the top of the outer core and can only cool by conduction into the surrounding mantle around its edges and upper surface.

The change in phase boundary due to chemistry, and its potential effects upon the effective position of the PPV phase boundary in chemically distinct regions in illustrated in Figure 4. In particular, we note that in the most general case material can host a single- or double-crossing scenario depending upon its chemistry, since the temperature of the phase boundary may be higher or lower than the CMB temperature at CMB pressure (~136 GPa). Matters could be even more complex than illustrated here, for example if material with different chemistry exhibits a different effective Clapeyron slope for the PPV transition and differently sized two-phase regions [*Spera, et al.*, 2006]. Some of the potential complexity introduced in this scenario is illustrated in Figure 3, where there are two differences between the upper and lower panels. The first difference is that in the upper panel there are no "holes" in the PPV bearing rock layer, as in this scenario the temperature is never hot enough to cause the layer of PPV to pinch out entirely as is the case in the lower panel. This depends on both the magnitude of lateral temperature

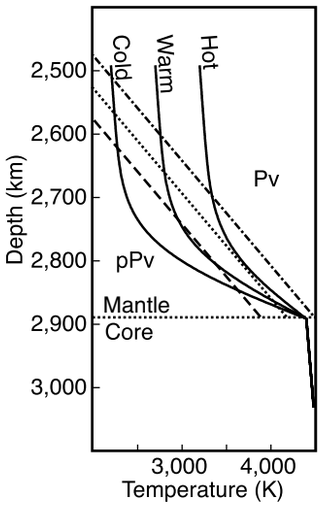

Figure 4. Geotherms and PPV phase boundaries for three different compositions (dashed, dotted and dot-dashed lines) and three different geotherms (labelled hot, warm and cold). For material with an effective phase boundary temperature higher than the CMB temperature (dot-dashed), a single-, rather than double-, crossing is expected. For a detailed explanation see text.

variations as well as the PPV Clapeyron slope, with the presence of holes arguing for larger temperature variations and/or Clapeyron slopes. The second difference is that in the upper panel, material inside the "piles" exhibits an effective single-crossing-like PPV phase boundary with a temperature at the CMB greater than that of the outermost isothermal core, while the lower panel still allows a double-crossing and formation of a post-perovskite lens inside the pile. The scenario illustrated in the lower panel is the one suggested by [*Lay, et al.*, 2006] who find strong evidence for a lens-like structure that pinches out laterally inside the Pacific low shear velocity province. The presence of lens-like features outside piles is also favored by [*van der Hilst, et al.*, 2007], who find a lens-like structure in their seismic migration of the Cocos region of D" which appears to pinch out laterally to the west. Therefore, the lower panel appears to be most consistent with the latest seismic observations, although in either case we note that a thicker PPV layer in the center of the "piles" along with its internal lateral temperature gradients should help drive an active component of flow which is correlated with ordinary counter-circulation.

Finally, PPV is shown in a thin basal layer, which applies if material hosting a single-crossing-like PPV phase exists in the chemically-distinct ULVZ scenario discussed above, as suggested by [*Mao, et al.*, 2006]. In this case, the reversion to perovskite phase at shallower depths occurs due to a change in composition with height rather than pressure-temperature variations alone, and opens the possibility for a "triple-crossing" as illustrated in Figure 3. [*Mao, et al.*, 2006] have argued that a dense Fe-rich silicate rock could host PPV and explain some of the anomalous seismic properties of ULVZ without requiring the presence of partial melt [*Williams and Garnero*, 1996], although it remains to be demonstrated whether a rock with the high Fe contents of these experiments remains solid at realistic CMB temperatures. Furthermore, recent studies of large Fe content $(Mg,Fe)SiO_3$ find that Fe stabilizes PV instead of PPV [*Tateno, et al.*, 2007], presenting a conflict that needs to be resolved before any interpretations of the stable phases in a basal Fe-rich layer can be made.

In Figure 3, some local complexity is illustrated inside a subducting slab, which could host small-scale variations in the distribution of PPV due to the relatively fine layering of MORB and harzburgite. The relative variations in phase boundary pressure in each case is shown solely for illustrative purposes, and does not necessarily reflect robust mineral physics constraints, some of which are presently not in accord with one another, as discussed above and recently reviewed by [*Hirose*, 2006]. Small-scale complexity in slabs carries obviously important implications for the fine-seismic structure of any subducted slabs in D" [*Hutko, et al.*, 2006; *van der Hilst, et al.*, 2007], yet it remains to be seen whether this kind of effect will carry any important dynamical consequences or whether an average treatment such as those in present mantle convection models with PPV adequately captures the basic dynamics.

Other dynamical issues that need further investigation include the suggestion that the lower phase boundary in the double-crossing scenario might itself be unstable [*Lay, et al.*, 2006]. This kind of instability may take the form of small-scale circulation leading to corrugations in the phase boundary interface, which would in turn carry consequences for its seismic signature at short wavelengths. Instabilities at the PPV interface can also be affected by lateral chemical variations since these both affect the position of the phase boundary and should also exhibit intrinsic density variations [*Spera, et al.*, 2006]. However, this kind of dynamically generated structure will be strongly influenced by viscosity variations, which in current modeling studies are probably less than realistic. In any case, the dynamical setting for smaller-scale instability is also under-resolved in global scale mantle convection studies, and regional scale studies might be better capable of addressing these issues in the future.

5.3. Outlook

Despite the present challenges facing more realistic modeling of PPV phase change behavior as well as issues that must be addressed by mineral physics in better understanding chemical as well as thermal modulation of the phase boundary, there is room for a great deal of important progress in the

future study of the PPV phase change. Other issues that may be further addressed include dynamical and seismological constraints on the morphology of the PPV-bearing rock layer that can better reveal both thermal and compositional variations as well as the style of mantle convection. For example, whether the layer contains holes but otherwise forms a connected network like a "swiss cheese" topology, or if PPV-lenses exist as unconnected islands like a "meat ball" topology, can potentially lend important insight into the planform of convection in the deep mantle that can be more directly constrained by observations. Combined experimental constraints on the PPV phase boundary in various compositions may also help distinguish exactly what kind of compositional variations are present in various seismic structures, particularly if the phase behavior is significantly different in candidate compositions. Last, but not least, we note the important constraints that this phase change offers regarding CMB heat flow, a quantity of first-order importance for the dynamo and in understanding the thermal evolution of Earth.

Acknowledgments. The authors thank Marc Monnereau for a thoughtful review.

REFERENCES

Breuer, D., H. Zhou, D. A. Yuen, and T. Spohn (1996), Phase-Transitions In the Martian Mantle - Implications For the Planets Volcanic History, *Journal Of Geophysical Research Planets*, *101*, 7531-7542.

Christensen, U. R., and A. W. Hofmann (1994), Segregation of subducted oceanic crust In the convecting mantle, *J. Geophys. Res.*, *99*, 19867-19884.

Christensen, U. R., and D. A. Yuen (1985), Layered convection induced by phase transitions, *J. Geophys. Res.*, *90*, 10291-10300.

Deschamps, F., J. Trampert, and P. J. Tackley (2007), Thermo-chemical structure of the lower mantle: seismological evidence and consequences for geodynamics, in *Superplume: Beyond Plate Tectonics*, edited by D. A. Yuen, et al., p. in press, Springer.

Harder, H. (1998), Phase transitions and the three-dimensional planform of thermal convection in the Martian mantle, *J. Geophys. Res. (USA)*, *103*, 16775-16797.

Harder, H., and U. R. Christensen (1996), A One-Plume Model Of Martian Mantle Convection, *Nature (UK)*, *380*, 507-509.

Hernlund, J., and S. Labrosse (2007), Geophysically consistent values of the perovskite to postperovskite transition Clapeyron slope, *Geophys. Res. Lett.*, *34*, doi:10.1029/2006GL028961.

Hernlund, J. W., C. Thomas, and P. J. Tackley (2005), A doubling of the post-perovskite phase boundary and structure of the Earth's lowermost mantle, *Nature (UK)*, *434*, 882-886.

Hirose, K. (2006), Postperovskite phase transition and its geophysical implications, *Rev. Geophys.*, *44*, doi: 10.1029/2005RG000186.

Hirose, K., R. Sinmo, N. Sata, and Y. Ohishi (2006), Determination of post-perovskite phase transition boundary in MgSiO3 using Au and MgO pressure standards, *Geophys. Res. Lett.*, *33*, doi:10.1029/2005GL024468.

Hutko, A., T. Lay, E. Garnero, and J. S. Revenaugh (2006), Seismic detection of folded, subducted lithosphere at the core-mantle boundary, *Nature (UK)*, *441*, 333-336.

Ishii, M., and J. Tromp (1999), Normal-mode and free-air gravity constraints on lateral variations in velocity and density of Earth's mantle, *Science (USA)*, *285*, 1231-1235.

Kageyama, A., and T. Sato (2004), The "Yin-Yang grid": An overset grid in spherical geometry, *Geochem. Geophys. Geosyst.*, *5*, doi:10.1029/2004GC000734.

Kameyama, M., and D. A. Yuen (2006), 3-D convection studies on the thermal state in the lower mantle with post-perovskite phase transition, *Geophys. Res. Lett.*, *33*, doi:10.1029/2006GL025744.

Lay, T., and E. J. Garnero (2004), Core-mantle boundary structures and processes, in *The State of the Planet: Frontiers and Challenges in Geophysics*, edited by R. S. J. Sparks and C. J. Hawkesworth, p. doi:10.1029/1150GM1004, AGU, Washington, D. C.

Lay, T., E. J. Garnero, and Q. Williams (2004), Partial melting in a thermo-chemical boundary layer at the base of the mantle, *Phys. Earth Planet. Int.*, *146*, 441-467.

Lay, T., and D. V. Helmberger (1983), A shear velocity discontinuity in the lower mantle, *Geophys. Res. Lett.*, *10*, 63-66.

Lay, T., J. Hernlund, E. J. Garnero, and M. S. Thorne (2006), A post-perovskite lens and D" heat flux beneath the central Pacific, *Science (USA)*, *314*, 1272-1276.

Mao, W. L., et al. (2006), Iron-rich postperovskite and the origin of ultralow-velocity zones, *Science (USA)*, *312*, 564-565.

Mao, W. L., et al. (2004), Iron-rich silicates in the Earth's D" layer, *Proc. Natl. Acad. Sci.*, *102*, 9751-9753.

Masters, G., G. Laske, H. Bolton, and A. Dziewonski (2000), The relative behavior of shear velocity, bulk sound speed, and compressional velocity in the mantle: Implications for chemical and thermal structure., in *Geophysical Monograph on Mineral Physics and Seismic Tomography fom the atomic to the global scale*, edited by S. Karato, et al., pp. 63-87, Americal Geophysical Union.

Matyska, C., and D. A. Yuen (2005), The importance of radiative heat transfer on superplumes in the lower mantle with the new post-perovskite phase change, *Earth Planet. Sci. Lett.*, *234*, 71-81.

McNamara, A. K., and S. Zhong (2005), Thermochemical piles beneath Africa and the Pacific Ocean, *Nature (UK)*, *437*, 1136-1139.

Murakami, M., K. Hirose, K. Kawamura, N. Sata, and Y. Ohishi (2004), Post-perovskite phase transition in $MgSiO_3$, *Science (USA)*, *304*, 855-858.

Nakagawa, T., and P. J. Tackley (2004a), Effects of a perovskite-post perovskite phase change near the core-mantle boundary on compressible mantle convection, *Geophys. Res. Lett.*, *31, L16611*, doi:10.1029/2004GL020648.

Nakagawa, T., and P. J. Tackley (2004b), Effects of thermo-chemical mantle convection on the thermal evolution of the Earth's core, *Earth Planet. Sci. Lett.*, *220*, 107-119.

Nakagawa, T., and P. J. Tackley (2004c), Thermo-chemical structure in the mantle arising from a three-components convective system and implications for geochemistry, *Phys. Earth Planet. Inter.*, *146*, 125-138.

Nakagawa, T., and P. J. Tackley (2005a), Deep mantle heat flow and thermal evolution of Earth's core in thermo-chemical multiphase models of mantle convection, *Geochem., Geophys., Geosys.*, *6*, doi:10.1029/2005GC000967.

Nakagawa, T., and P. J. Tackley (2005b), The interaction between the post-perovskite phase change and a thermo-chemical boundary layer near the core-mantle boundary, *Earth Planet. Sci. Lett.*, *238*, 204-216.

Nakagawa, T., and P. J. Tackley (2006), Three-dimensional structures and dynamics in the deep mantle: Effects of post-perovskite phase change and deep mantle layering, *Geophys. Res. Lett.*, *33*, doi:10.1029/2006GL025719.

Ni, S., E. Tan, M. Gurnis, and D. V. Helmberger (2002), Sharp sides to the African superplume, *Science (USA)*, *296*, 1850-1852.

Oganov, A. R., and S. Ono (2004), Theoretical and experimental evidence for a post-perovskite phase of $MgSiO_3$ in Earth's D" layer, *Nature (UK)*, *430*, 445-448.

Olson, P., and C. Kincaid (1991), Experiments on the interaction of thermal convection and compositional layering at the base of the mantle, *J. Geophys. Res.*, *96*, 4347-4354.

Ono, S., A. R. Oganov, and Y. Ohishi (2005), In situ observations of phase transition between perovskite and $CaIrO_3$-type phase in $MgSiO_3$ and pyrolitic mantle composition, *Earth Planet. Sci. Lett.*, *236*, 914-932.

Rost, S., E. J. Garnero, Q. Williams, and M. Manga (2005), Seismic constraints on a possible plume root at the core-mantle boundary, *Nature (UK)*, *435*, 666-669.

Schubert, G., and D. L. Turcotte (1971), Phase transitions and mantle convection, *J. Geophys. Res.*, *76*, 1424-1432.

Schubert, G., D. A. Yuen, and D. L. Turcotte (1975), Role of phase transitions in a dynamic mantle, *J. R. Astron. Soc.*, *42*, 705-735.

Sidorin, I., M. Gurnis, and D. V. Helmberger (1999), Dynamics of a phase change at the base of the mantle consistent with seismological observations, *J. Geophys. Res.*, *104*, 15005-15024.

Spera, F. J., D. A. Yuen, and G. Giles (2006), Tradeoffs in chemical and thermal variations in the post-perovskite transition: Mixed phase regions in the deep lower mantle? *Phys. Earth Planet. Int.*, *159*, 234-246.

Stackhouse, S., J. Brodholt, and G. D. Price (2006), Elastic anisotropy of FeSiO3 end-members of the perovskite and post-perovskite phases, *Geophys. Res. Lett.*, *33*, doi:10.1029/2005GL023887.

Steinbach, V., D. A. Yuen, and W. L. Zhao (1993), Instabilities From Phase-Transitions and the Timescales Of Mantle Thermal Evolution, *Geophys. Res. Lett. (USA)*, *20*, 1119-1122.

Tackley, P. J. (1993), Effects of strongly temperature-dependent viscosity on time-dependent, 3-dimensional models of mantle convection, *Geophys. Res. Lett.*, *20*, 2187-2190.

Tackley, P. J. (1996), Effects of strongly variable viscosity on three-dimensional compressible convection in planetary mantles, *J. Geophys. Res.*, *101*, 3311-3332.

Tackley, P. J. (1998), Three-dimensional simulations of mantle convection with a thermochemical CMB boundary layer: D"? in *The Core-Mantle Boundary Region*, edited by M. Gurnis, et al., pp. 231-253, American Geophysical Union.

Tackley, P. J. (2002), Strong heterogeneity caused by deep mantle layering, *Geochem. Geophys. Geosystems*, *3*, 10.1029/2001GC000167.

Tackley, P. J., D. J. Stevenson, G. A. Glatzmaier, and G. Schubert (1993), Effects of an endothermic phase transition at 670 km depth in a spherical model of convection in the Earth's mantle, *Nature (UK)*, *361*, 699-704.

Tackley, P. J., D. J. Stevenson, G. A. Glatzmaier, and G. Schubert (1994), Effects of multiple phase transitions in a 3-dimensional spherical model of convection in Earth's mantle, *J. Geophys. Res.*, *99*, 15877-15901.

Tackley, P. J., and S. Xie (2003), Stag3D: A code for modeling thermo-chemical multiphase convection in Earth's mantle, paper presented at Second MIT Conference on Computational Fluid and Solid Mechanics, Elsevier, MIT.

Tateno, S., K. Hirose, N. Sata, and Y. Ohishi (2007), Solubility of FeO in (Mg,Fe)SiO3 perovskite and the post-perovskite phase transition, *Phys. Earth Planet. Int.*, *160*, 319-325.

Thomas, C., E. J. Garnero, and T. Lay (2004a), High-resolution imaging of lowermost mantle structure under the Cocos plate, *J. Geophys. Res.*, *109*, doi:10.1029/2004JB003013.

Thomas, C., J. M. Kendall, and J. Lowman (2004b), Lower-mantle seismic discontinuities and the thermal morphology of subducted slabs, *Earth Planet. Sci. Lett.*, *225*, 105-113.

Trampert, J., F. Deschamps, J. S. Resovsky, and D. Yuen (2004), Probabilistic tomography maps significant chemical heterogeneities in the lower mantle, *Science (USA)*, *306*, 853-856.

Tsuchiya, J., T. Tsuchiya, and R. M. Wentzcovitch (2005), Vibrational and thermodynamic properties o MgSiO3 postperovskite, *J. Geophys. Res.*, *110*, doi:10.1029/2004JB003409.

Tsuchiya, T., J. Tsuchiya, K. Umemoto, and R. A. Wentzcovitch (2004a), Phase transition in MgSiO3 perovskite in the earth's lower mantle, *Earth & Planetary Science Letters*, *224*, 241-248.

Tsuchiya, T., J. Tsuchiya, K. Umemoto, and R. M. Wentzcovitch (2004b), Elasticity of post-perovskite MgSiO3, *Geophys. Res. Lett. (USA)*, *31*, doi:10.1029/2004GL020278.

van der Hilst, R. D., et al. (2007), Seismo-stratigraphy and thermal structure of the Earth's core-mantle boundary region, *Science (USA)*, *in press*.

van Keken, P. (2001), Cylindrical scaling for dynamical cooling models of the Earth, *Phys. Earth Planet. Inter. (Netherlands)*, *124*, 119-130.

Weinstein, S. A. (1995), The Effects Of a Deep Mantle Endothermic Phase-Change On the Structure Of Thermal-Convection In Silicate Planets, *Journal Of Geophysical Research Planets*, *100*, 11719-11728.

Wen, L. (2001), Seismic evidence for a rapidly-varying compositional anomaly at the base of the Earth's mantle beneath the Indian ocean, *Earth Planet. Sci. Lett.*, *194*, 83-95.

Wen, L. X. (2002), An SH hybrid method and shear velocity structures in the lowermost mantle beneath the central Pacific and South Atlantic Oceans, *Journal of Geophysical Research-Solid Earth*, *107*, doi:10.1029/2001JB000499.

Williams, Q., and E. J. Garnero (1996), Seismic Evidence For Partial Melt At the Base Of Earths Mantle, *Science (USA)*, *273*, 1528-1530.

Xie, S., and P. J. Tackley (2004a), Evolution of helium and argon isotopes in a convecting mantle, *Phys. Earth Planet. Inter.*, *146*, 417-439.

Xie, S., and P. J. Tackley (2004b), Evolution of U-Pb and Sm-Nd systems in numerical models of mantle convection, *J. Geophys. Res.*, *109, B11204*, doi:10.1029/2004JB003176.

Zhou, H., D. Breuer, D. A. Yuen, and T. Spohn (1995), Phase-Transitions In the Martian Mantle and the Generation Of Megaplumes, *Geophys. Res. Lett. (USA)*, *22*, 1945-1948.